Journal of Environmental Management 368 (2024) 122171

Contents lists available at ScienceDirect

Journal of Environmental Management

journal homepage: www.elsevier.com/locate/jenvman

Research article

Microalgal-based carbon encapsulated iron nanoparticles for the removal of pharmaceutical compounds from wastewater

Marco Mantovani *, Elena Collina, Elena Passalacqua, Marina Lasagni, Valeria Mezzanotte

Università degli Studi di Milano – Bicocca, Department of Earth and Environmental Sciences (DISAT), P.zza della Scienza 1, 20126, Milano, Italy

ARTICLE INFO

Keywords:
Novel adsorbent
Wastewater treatment
hydrothermal carbonization
Microalgae biomass
Micropollutants

ABSTRACT

This study evaluates the effectiveness of microalgal-based carbon-encapsulated iron nanoparticles (ME-nFe) in the removal of pharmaceutical compounds (PhACs) from water solutions and real municipal effluent at a laboratory scale. The investigated PhACs were chosen to represent different classes of synthetic drugs: antibiotics, anti-inflammatory drugs, antihypertensives, antiepileptics, neuroprotectors, and antidepressants. The adsorbent material was produced through hydrothermal carbonization (225 °C for 3 h), using microalgae grown on wastewater as the carbon source. ME-nFe showed heterogeneity in terms of porosity (with both abundance of macro and mesopores), a total pore volume of 0.65 mL g^{-1}, a specific surface area of 117 m^2 g^{-1} and a total iron content of 40%. Laboratory scale adsorption tests (1 g L^{-1} of nanoparticles with 2 min contact time) showed high removal for the most hydrophobic compounds. Removal efficiencies were high (over 98%) for Irbesartan, Ofloxacin and Diclofenac, promising (over 65–80%) for Clarithromycin, Fluoxetine, Lamotrigine and Metoprolol, but low for Gabapentin-Lactam and Propyphenazone (<20%). Electrostatic interactions between the drugs and the surface of the nanoparticles may account for the observed data, although additional removal mechanisms cannot be ruled out.

1. Introduction

The contamination of natural water bodies by pharmaceutical compounds (PhACs) has become an issue of growing concern in recent years due to their widespread use and persistence in the environment (Adeleye et al., 2022). PhACs are designed to be biologically active at low concentrations and resist degradation, making them recalcitrant to conventional biological treatment methods (Luo et al., 2019; Silori and Tauseef, 2021). Municipal wastewater treatment plants (WWTPs) were not originally designed to address the removal of such contaminants. Therefore, the presence of PhACs in effluents poses a considerable challenge with potential environmental impacts. The continuous exposure of microorganisms to antimicrobial drugs promotes the development of antimicrobial resistance (AMR) among bacteria and pathogens (Frascaroli et al., 2021). This is not a minor issue, as AMR leads to the decreased efficacy of antimicrobials, prolongs diseases, and increases mortality (Skandalis et al., 2021). Advanced oxidation processes (AOPs), biological treatment, adsorption, and membrane filtration are among the most common technologies used for PhAC removal. Each of these approaches has its advantages and drawbacks. Their effectiveness can vary depending on the specific pharmaceutical compounds and operating conditions (Rodríguez-Serin et al., 2022). While significant progress has been made in pharmaceutical removal, several challenges persist. These include incomplete removal, the formation of transformation products with unknown toxicity, and the potential environmental release of active compounds due to treatment inefficiencies (Bollmann et al., 2016). An interesting approach could be the combination of processes with different mechanisms. Synergistic effects can be exploited, potentially leading to high efficiency in removing organic pollutants. Noudeh et al. combined electrocoagulation techniques with chitosan adsorption to remove antibiotics from hospital wastewater (Noudeh et al., 2023). Nowadays, adsorption is still considered the most readily scalable process, as AOPs involve higher operation costs (including both oxidants and energy requirements) and can potentially generate transformation products (Mirzaei et al., 2017). Activated carbons (ACs) are the most studied adsorbents given their large specific surface area (over 500 m^2g^{-1}) and pore volume. Pore size distribution is another interesting characteristic: while the abundance of micropores makes them potentially effective in the adsorption of high amounts of micropollutants, the uptake is usually slow (up to some hours) (Bhadra

* Corresponding author.
E-mail address: m.mantovani10@campus.unimib.it (M. Mantovani).

https://doi.org/10.1016/j.jenvman.2024.122171
Received 17 April 2024; Received in revised form 25 July 2024; Accepted 7 August 2024
Available online 11 August 2024

et al., 2016). Another drawback involves the management of the saturated ACs. Since effective regeneration strategies are still lacking, their disposal as harmful waste material is the most common approach. Moreover, the development of energy-efficient, cost-effective removal processes remains a priority as the concept of WWTP is evolving. In this context, emerging strategies involving the use of innovative materials such as nanoparticles and advanced adsorbents, produced from waste products or biomasses, are rising (Liu et al., 2023). The potential use of zero-valent iron nanoparticles (nZVI) in wastewater treatment has raised attention due to their high reactivity toward various contaminants. Properties such as their high surface area and redox potential make them effective agents for the degradation of micropollutants in water (Zou et al., 2016). Encapsulating these iron nanoparticles within a carbonaceous matrix further enhances their stability, reactivity, and overall performance in wastewater treatment applications, while reducing aggregation. The synergistic combination of iron nanoparticles and carbonaceous materials seems a promising avenue for addressing water pollution challenges (Fronczak et al., 2018). Iron-impregnated carbon nanotubes made from chitosan (MCS@MWCNTs) were recently proposed to remove acetaminophen from aqueous solutions. The combination of their nanosized structure (hollowed and layered) and the magnetic properties of Fe_3O_4 make them an effective and promising technology (Nabatian et al., 2022). Iron-based nanomaterials can also be employed in conjunction with AOPs, leveraging the activity of iron itself, which can replace more conventional catalysts (Olusegun et al., 2023). This could result in reduced process costs. Within this context, ZnO/Fe_2O_3 nanocomposite was studied to trigger the ozonation of Captopril from wastewater (Dolatabadi et al., 2022). Iron-loaded adsorbents can be produced through hydrothermal carbonization (HTC), working under relatively moderate temperature and pressure conditions (180–250 °C). The water content of many carbonaceous biomasses serves as a natural and cost-effective catalytic agent, playing a pivotal role in reducing the activation energy required for the different chain-like reactions occurring in the reactor. HTC can be used to produce carbon-coated iron nanoparticles or iron-loaded hydrochar (Gautam et al., 2024) by using biomasses or waste materials with reducing power, avoiding the use of harmful chemicals needed in other conventional synthesis methods (Calderon et al., 2018). Munoz et al. (2021) recently demonstrated the effectiveness of iron-loaded mesoporous carbon materials (CE-nFe) in the removal of a mixture of three PhACs (Diclofenac, Sulfamethoxazole and Metronidazole) from water solution at laboratory scale. A regeneration involving heterogeneous Fenton oxidation, exploiting the iron content of the adsorbent as a catalyst was also proposed.

This study concerns the laboratory-scale application of microalgal-based carbon-encapsulated iron nanoparticles (ME-nFe) for the removal of pharmaceutical compounds (PhACs) from a real wastewater effluent. Unlike many studies that use unrealistically high concentrations of contaminants, this research focuses on concentrations typically found in a municipal wastewater, ranging from a few nanograms per liter to micrograms per liter. The low concentrations and heterogeneity of emerging micropollutants are not just analytical challenges; they are major factors in the inefficiencies of conventional treatment methods. The research introduces an innovative approach involving microalgae grown on wastewater, directly harvested from a pilot microalgal pond within the Bresso-Niguarda wastewater treatment plant (WWTP) in Milan, Italy. These nanoparticles have proven to be quite versatile, given their effectiveness in removing certain heavy metals from the secondary effluent of the wastewater treatment plant (Mantovani et al., 2023). If they prove to be equally promising for treating organic contaminants from real wastewaters, the integration of microalgae into conventional WWTPs could gain more attention. As described by Rossi et al. (2023) microalgae and bacteria can be used as a side stream treatment to remove nitrogen, phosphorus, and organic matter from the liquid phase of anaerobic sludge. By reducing the loads of these nutrients in the supernatant before it is redirected at the beginning of the wastewater treatment line, it is possible to reduce the energy costs of the WWTP related to mechanical oxygenation in activated sludge systems (Tua et al., 2021). The biomass grown on the wastewater can then be separated and processed through HTC to produce microalgal-based iron nanoparticles. These nanoparticles could be directly employed in the WWTP and used for polishing the effluent, removing heavy metals and pharmaceutical residues either in substitution or in addition to the already designed or existing tertiary treatments. Compared to conventional powdered activated carbons, these nanoparticles are faster adsorbents that exhibit both reducing power and magnetic properties due to the presence of iron. This would allow for their recovery after treatment without the need for centrifugation processes. If WWTPs were to adopt this technology, using algae biomass grown directly onsite, they could potentially enhance the efficiency and effectiveness of the treatment chain (Mezzanotte et al., 2022).

2. Material and methods

2.1. Chemicals

Iron (III) nitrate nonahydrate ($Fe(NO_3)_3{\cdot}9H_2O$)) (Sigma-Aldrich) was used as the iron source for the production of the ME-nFe. Ethanol (Sigma-Aldrich) was used to wash the nanoparticles after the synthesis. Amisulpride (AMS), Ofloxacin (OFX), Metoprolol (MTP), Sulfamethoxazole (SFX), Clarithromycin (CLM), Gabapentin-Lactam (GBP), Carbamazepine (CBZ), Irbesartan (IRB), Diclofenac (DCN), Lamotrigine (LMG), Fluoxetine (FLX) and Propyphenazone (PHP) were purchased in their solid forms (Sigma-Aldrich). Methanol, formic acid and Ultrapure water (UW) (Sigma-Aldrich) were used to prepare the mobile phases to detect the PhACs through UPLC-MS.

2.2. ME-nFe production

Microalgae grown on wastewater were used as the source material for the HTC process to produce microalgal-based carbon-encapsulated iron nanoparticles (ME-nFe). The biomass was grown in a pilot-scale high-rate algae-bacteria pond (HRAP) situated at the Bresso-Niguarda Wastewater Treatment Plant (WWTP) in the outskirts of Milan, Italy. A mixed culture primarily composed of *Chlorella vulgaris* and *Scenedesmus* spp. (*S. acutus, S. obliquus and S. acuminatus*) was cultivated on the liquid phase of anaerobic sludge, called centrate (as it is obtained through centrifugation) (Rossi et al., 2023). This cultivation was conducted continuously for eight months (from May to November 2021), serving as a pilot-scale treatment to remove nitrogen and phosphorus. The microalgae were harvested directly at the Bresso plant using an ELECREM 1110/230 V centrifugal clarifier. Raw samples of the microalgal suspension were collected to perform total suspended solids (TSS) analysis according to Standard Methods (APHA/AWWA/WEF, 2012). 10 L of the microalgal suspension was centrifuged and the fresh biomass was preserved in a glass bottle and stored in the fridge before being used. The ME-nFe were obtained with a single-step process through hydrothermal carbonization following the protocol described in a previous work (Mantovani et al., 2023), slightly modified. Fresh biomass was used instead of the freeze-dried one. The microalgal pellet obtained through centrifugation was re-suspended in 200 mL of distilled water. Considering the starting TSS concentration in the HRAP (0.6 $gTSS{\cdot}L^{-1}$), a 30 $gTSS{\cdot}L^{-1}$ was obtained and enriched with 15 g of $Fe(NO_3)_3{\cdot}9H_2O$. Then, the microalgal and iron salt mixture was transferred to a High-Pressure Laboratory Reactor (BR-700, BERGHOF) and heated to the end temperature of 225 °C (Fig. 1S of Supplementary Material). An autogenous pressure of 30 bar was generated as a consequence of the gas and aqueous vapour inside the reactor. During the process, chain chemical reactions are responsible for the de-structuration of the microalgal carbonaceous matrix (Wang et al., 2018) and the reduction of the iron salt. These lead to the formation of iron nanoparticles (both iron oxides and zero-valent iron) that are encapsulated inside the

carbonaceous matrix. After that, the reactor was left to cool overnight. Finally, the HTC products (liquid and solid) were recovered and separated by vacuum filtration using a cellulose acetate filter (cut-off 0.2 μm). The solid fraction (ME-nFe) was subsequently washed three times with a 50:50 (v:v) water-ethanol solution, removing the tar and other HTC residues and dried at 80 °C for 12 h. Finally, it was ground and stored in a glass vial.

2.3. ME-nFe characterization

The nanoparticles were characterized to better understand their properties following different techniques. BET surface area and the pore size distribution analysis on the ME-nFe were obtained by physical adsorption on the solid surface of nitrogen gas molecules at 77 K, by a Coulter SA 3100 analyzer at Università degli Studi di Milano. The method for measuring the specific surface area ($m^2 \cdot g^{-1}$) of the material is based on the theory developed by Brunauer, Emmett and Teller (BET). The size and morphology of the nanoparticles were evaluated through a LEO 1430 Scanning Electron Microscope (SEM). TEM images were acquired with JEOL JEM 2100Plus Transmission Electron Microscope (JEOL, Japan) operating with an acceleration voltage of 200 kV and equipped with an 8-megapixel Gatan (Gatan, USA) Rio Complementary Metal-Oxide-Superconductur (CMOS) camera. Energy dispersive X-ray (EDX) analyses were performed on a Hitachi TM 1000 scanning electron microscope to check the atomic composition of the nanoparticles. Microwaved-assisted acid digestion following Inductively Coupled Plasma-Optical Emission Spectroscopy (Optima 7000 DV PerkinElmer) was performed to investigate the total iron content of the material. The crystalline phases were analyzed by X-ray diffraction (XRD) using an X-ray powder diffractometer PANalytical X'Pert PRO PW3040/60 with Cu radiation at 40 kV with a step size of step 0.02° at 2 s/step. The functional groups of the samples were analyzed by micro-FTIR (Thermo Fisher, Nicolet IN10). The determination of the point of zero charge (PZC) by the pH drift method was carried out according to (Bhattarai et al., 2020). A NaCl 0.01M stock solution was boiled in a glass beaker to remove dissolved CO_2. Multiple 20 mL aliquots of this solution were sampled and put into 50 mL Falcons. The pH of each sample was adjusted to consecutive integers ranging from 2 to 10 using 1M HCl and 0.1M NaOH solutions. Subsequently, ME-nFe nanoparticles were weighed (150 mg) and added to each Falcon. The sealed samples were put on a horizontal shaker for 24 h. Finally, the nanoparticles were removed from the solutions by filtration and pH was measured using a pH-meter (XS INSTRUMENTS mod—PC 510). For each sample, the final pH value (pH_{24h}) was recorded and plotted against the starting value (pH_0). The PZC refers to the intersection point between the curve connecting individual data points and the $pH_0 = pH_{24h}$ line, indicating the pH of the solution where the nanoparticles exhibit an overall neutral surface charge.

2.4. Application of ME-nFe nanoparticles for the removal of PhACs

Microalgal-based carbon encapsulated zero-valent iron nanoparticles (ME-nFe), produced through hydrothermal carbonization (HTC) were used as adsorbents to remove 12 pharmaceutical compounds from water solutions and a municipal treated effluent (from Bresso WWTP). A VELP FC 6S Jar tester and 500 mL beakers were used, under 90 rpm continuous stirring. Preliminarily, adsorption tests were performed on a synthetic solution containing all the PhACs at a starting concentration of 1.5 μg L^{-1}. Three doses of nanoparticles were tested (0.1, 1, and 3 g L^{-1}) as well as two contact times (2 and 10 min). This configuration was chosen according to similar applications found in the literature. Specifically, these short contact times were selected following an evaluation of the adsorption kinetics of similar nanoparticles for Diclofenac, Sulfamethoxazole, and Metronidazole (Munoz et al., 2021). By 5 min, 90% of the equilibrium uptake had been achieved. Based on the best results (1 g ME-nFe·L^{-1} dose and 2 min contact time) a similar adsorption test was performed on the effluent from Bresso WWTP (instead of the synthetic solution) investigating the effectiveness of the ME-nFe on the same targeted PhACs. Effluent samples were collected before the UV disinfection process (pre-UV). At the end of the tests, the nanoparticles were separated from the liquid phase using a neodymium magnet, holding them at the bottom of the beaker while siphoning the solution into a clean one. All experiments on the synthetic solution were carried out in quintuplicate while the effluent ones were performed in triplicate. The removal efficiencies of pharmaceuticals (η_X) were computed according to the following formula:

$$\eta_X = \frac{(X_u)-(X_t)}{(X_u)} \quad (1)$$

Where: X_u and X_t are the concentrations of the compound X in the untreated and treated samples, respectively.

2.5. PhACs and analytical procedure

Amisulpride (AMS), Ofloxacin (OFX), Metoprolol (MTP), Sulfamethoxazole (SFX), Clarithromycin (CLM), Gabapentin-Lactam (GBP), Carbamazepine (CBZ), Irbesartan (IRB), Diclofenac (DCN), Lamotrigine (LMG), Fluoxetine (FLX) and Propyphenazone (PHP) were the target PhACs. They belong to different classes of synthetic active compounds, and they are commonly detected in municipal wastewater. Except for CLM which is a larger molecule, all the others have similar molar masses. Some of them (CBZ, IRB, DCN, LMG, FLX, OFX, and CLM) have hydrophobic properties while others (GBP, AMS, SFX, PHP and MTP) have high hydrophilicity (more information on Table 1S of Supplementary Material). Starting from solid standards, a 1000 μg L^{-1} stock solution containing all the analytes (solution A) was prepared according to Mantovani et al. (2024). Solution A was used to prepare the calibration curves for each compound (with seven calibration points between 0.5 and 50 ng mL^{-1}) and the synthetic solutions for the adsorption tests. Limits of detection (LODs) and quantification (LOQs) were determined as threefold and tenfold the standard deviation of the lowest standard, as indicated in the ISO 6107:2021 Standard (ISO, 2021) (More information can be found in Supplementary Material, Tables 2S–4S). Similarly, an internal standard (IS) working solution of 1000 μg L^{-1} of fluoxetine-d6 was prepared. The 1.5 μg L^{-1} synthetic solutions for the first series of tests were prepared by adding 375 μL of solution A in 250 mL of ultrapure water (UW). After the adsorption test, the ME-nFe were recovered using a neodymium magnet while the water samples were filtrated (cutoff 0.2-μm) and stored in autosampler vials, ready to be analyzed. A sample of untreated solution was also collected. Concerning the application of ME-nFe on Pre-UV effluents, 120 mL of treated wastewater were collected and filtered at 0.2 μm. Later the samples were spiked with 2.5 μL of the IS solution. The same process was carried out for procedural blanks using UW. Both treated and untreated samples were collected and underwent a solid-phase extraction process using Oasis® HLB cartridges (200 mg/6 mL, Waters, Milford, MA). The pre-concentration protocol involved the following steps: conditioning the cartridges with 6 mL of methanol and 6 mL of UW, vacuum filtration extraction at a rate of 5–10 mL min^{-1}, washing with 6 mL of UW, followed by a 15-min air-drying. Elution was performed using 6 mL of methanol. Subsequently, the obtained samples were concentrated under a nitrogen stream, resuspended in 1 mL of UW, and transferred to autosampler vials. The separation process was made by an XSelect CSH C18 XP chromatographic column (130 Å, 2.5 μm, 3 mm × 100 mm) with solvent A (UW with 1 mM ammonium acetate and 0.10% formic acid) and solvent B (methanol with 1 mM ammonium acetate and 0.10% formic acid) as mobile phases. The analysis was carried out using ultra-performance liquid chromatography (Acquity UPLC H-class, Waters, USA) coupled with a QDa detector (Waters, USA), with elution rates adjusted based on the specific compounds being analyzed. The flow rate was maintained at 0.5 mL min^{-1}.

3. Results and discussion

3.1. Characterization of microalgal-based carbon-encapsulated iron nanoparticles

Fig. 1A shows the SEM image of the nanoparticles, which had a globular morphology consistent with the one described in Mantovani et al. (2023), obtained from the same microalgal biomass (Fig. 1B). A better visual of the sample can be obtained by TEM images. ME-nFe appears aggregated as to be expected from a material obtained through HTC. The microalgal biomass subjected to the HTC process tends to undergo structural breakdown, forming hydrochar (Fig. 1C). This leads to the formation of particles and aggregates of large dimensions (up to a few microns), within which the small iron nanoparticles are encapsulated and can be distinguished, especially at higher magnifications (Fig. 1D). The Average diameter of iron nanoparticles (9 ± 3 nm) was determined through imageJ software. The specific surface area (BET) of the ME-nFe was 117 $m^2\ g^{-1}$, similar to other novel adsorbents produced through hydrothermal carbonization ((Calderon et al., 2018; Munoz et al., 2021)), but lower than the one obtained after the pyrolysis (750 °C) of iron-loaded microalgae (201 $m^2\ g^{-1}$) (Nakarmi et al., 2022). The higher temperature of pyrolysis in the absence of oxygen likely led to increased loss of the carbonaceous matrix and the formation of more defective sites, consequently resulting in a higher specific surface area. This parameter is important as it describes the potential adsorption capacity of the ME-nFe. The nitrogen adsorption isotherm (Fig. 2A) showed no hysteresis loop, having a shape that can be assimilated to the type II of IUPAC classification. This kind of adsorption isotherm usually describes nonporous or macroporous material. Fig. 2B shows the pore size distribution of ME-nFe, calculated using the Barret-Joyner-Halenda (BJH) method based on the desorption branches of the isotherm. Actually, 42 % of the total pore volume was made of macropores having a diameter higher than 80 nm. Mesopores were only slightly less abundant (38% of the total pore volume had a diameter ranging from 20 to 80 nm) while micropores (diameter <6 nm) accounted for approximately 10%. The presence of mesopores is important. They ensure faster adsorption of micropollutants than microporous materials such as activated carbon, which usually need long times (up to hours) due to diffusion limitations. Reduced contact times for adsorption would enhance the efficiency and practicality of tertiary wastewater treatment (Xiao and Hill, 2017). The total pore volume accounted for 0.65 mL g^{-1}. The material's total iron content was 39.5% by weight and was quantified using ICP after acid digestion. Assuming a homogeneous distribution of iron within the nanoparticles and considering the yield obtained in their production, the 4 g of ME-nFe recovered from a single HTC batch contained 1.6 g of iron. Each synthesis uses 15 g of Fe $(NO_3)_3{\cdot}9H_2O$, corresponding to 2.06 g of iron. This results in an iron incorporation efficiency into the carbonaceous matrix of approximately 78%. The result of EDX analysis is illustrated in Fig. 3S of Supplementary Material, confirming the relevant presence of iron and showing an abundance of oxygen (38 and 37 % wt., respectively). This suggests that iron oxides could be rather relevant in the ME-nFe, while carbon accounted for 21% wt. The material was also composed of less abundant elements such as aluminum, phosphorus and silica (0.5, 0.3 and 2.7 % wt., respectively). The first ones are common elements of green microalgal biomass, while Si could be attributed to the presence of *Diatoms* (a peculiar taxon of brown microalgae characterized by a silica shell) that can be found in small concentration in the microalgal community of Bresso pilot raceway. The XRD pattern confirmed the presence of iron oxide (Fig. 4S of Supplementary Material) showing the crystalline phase of hematite (Fe_2O_3, at 33.1°, 35.6°, 40.8°, 49.4°, 54.0° and 64.0°) and magnetite (Fe_3O_4 at 30.0°). The functional groups on the surface of ME-nFe were determined by FTIR analysis. As shown in Fig. 6S of Supplementary Material, a broad peak around 3400-3200 cm^{-1} can be observed, revealing O-H stretching, typical of hydroxyl groups in alcohols and phenols. Peaks around 2950-2850 cm^{-1} indicate aliphatic

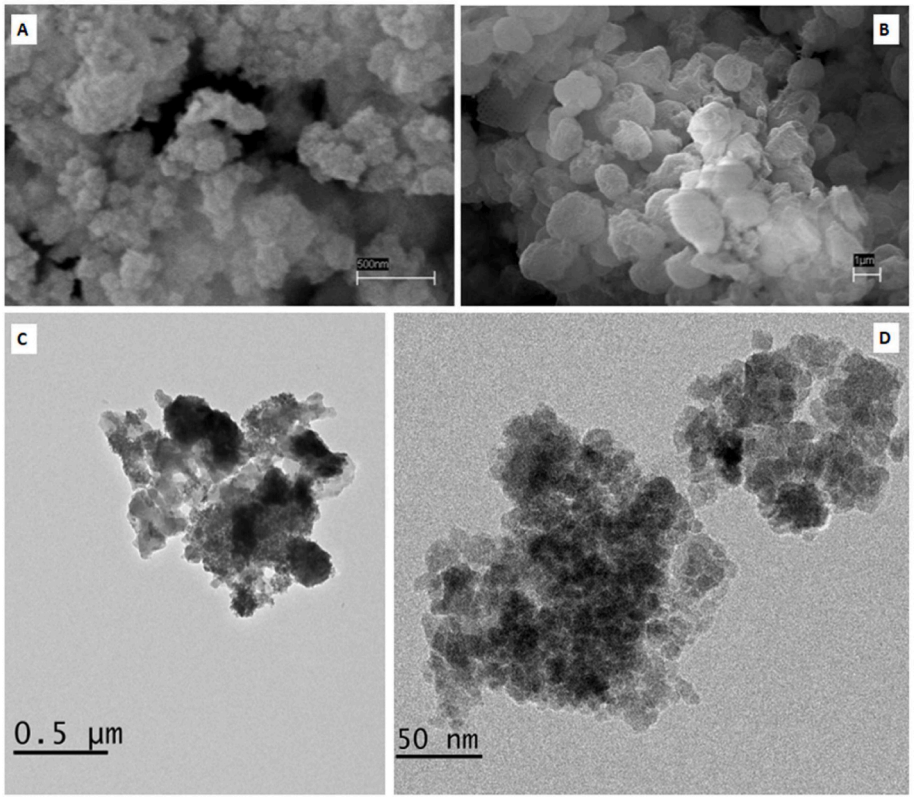

Fig. 1. SEM image of the ME-nFe (A); SEM image of freeze-dried microalgae used for the ME-nFe production (B); TEM images of ME-nFe at different levels of magnification (C and D).

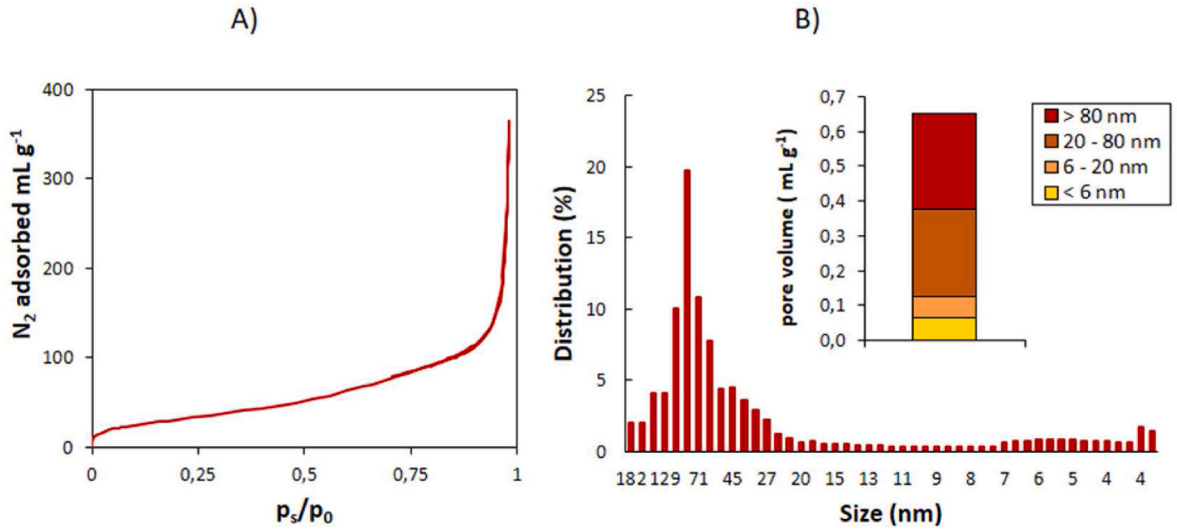

Fig. 2. Nitrogen adsorption-desorption isotherm of ME-nFe (A); Pore size distribution of ME-nFe(B).

C-H stretching vibrations, related to the methyl and methylene groups of fatty acids, suggesting the presence of alkane groups. The strong peak near 1700 cm^{-1} (1750-1650 cm^{-1}) reveals the presence of carbonyl groups (C=O), indicative of ketones, aldehydes, or carboxylic acids. To complete the ME-nFe characterization, the pH_{PZC} value was also measured at pH_{PZC} = 6.4 (Fig. 3S of Supplementary Material), which seemed consistent with literature data on iron oxide-loaded adsorbents (Noreen et al., 2020)

3.2. Application of ME-nFe nanoparticles for the removal of PhACs

Fig. 3 shows the results obtained in the first series of tests on the 1.5 μg L^{-1} solution varying the ME-nFe concentration and the adsorption time. The interaction with nanoparticles varied among different PhACs.

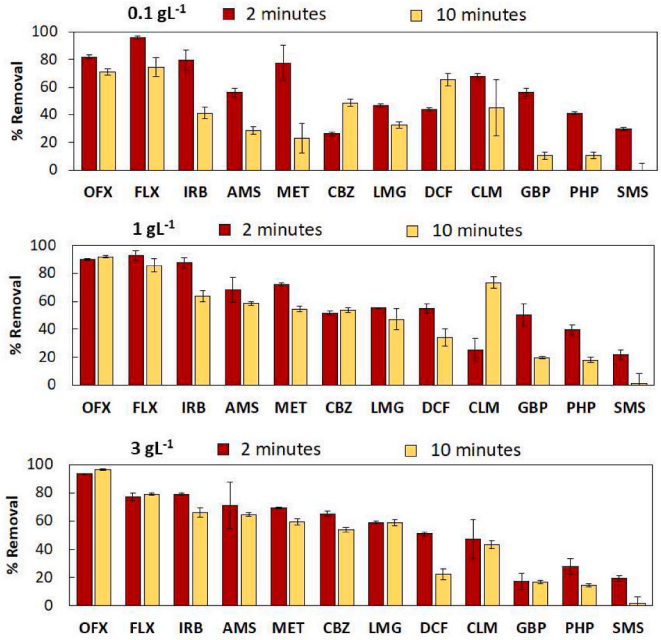

Fig. 3. Percent removal of Sulfamethoxazole (SMS), Lamotrigine (LMG), Diclofenac (DCF), Fluoxetine (FLX), Metoprolol (MET), Amisulpride (AMS), Ofloxacin (OFX), Carbamazepine (CBZ), Clarithromycin (CLM), Gabapentin-Lactam (GBP), Irbesartan (IRB), and Propyphenazone (PHP). Data are presented as average and standard deviations (n = 5).

For some of them, differences were highlighted based on the contact time, and the use of a higher adsorbent dose did not always result in greater removal. Overall, the shorter contact time (2 min) proved to be the most effective. Specifically, for Sulfamethoxazole (SMX), Gabapentin lactam (GBP), Propyphenazone (PHP), and Irbesartan (IBS), the residual concentrations were higher after 10 min compared to 2 min. This is likely associated with a partial desorption mechanism. On the other hand, the removal of Amisulpride (AMS), Ofloxacin (OFX), Metoprolol (MET), and Clarithromycin (CLM) was not affected by time, and no desorption occurred after 10 min. The lower dose of nanoparticles (0.1 g L^{-1}) was usually the least effective, except for Diclofenac (DCN). The differences observed between the tests at 1 g L^{-1} and 3 g L^{-1} are not so pronounced to justify the use of the higher dose. Furthermore, for some compounds (Gabapentin-lactam, Sulfamethoxazole, Propyphenazone and Fluoxetine), the removal efficiency was better at 1 g L^{-1}. This seems peculiar: increasing the ME-nFe dosage should enhance the number of active sites and improve efficiency unless aggregation phenomena among the nanoparticles did occur. To mitigate this potential issue, the subsequently used nanoparticles were homogenized using a sieve (cut-off 38 μm).

The analysis of the effluent from Bresso WWTP highlights a certain heterogeneity in the concentrations of the studied PhACs, from a few nanograms per liter (ng·L^{-1}) to micrograms per liter (μg·L^{-1}). On the other end, Sulfamethoxazole (SFX) and Carbamazepine (CBZ) concentrations were below their detection limits even after the SPE procedure, so they were not considered during the adsorption test (Table 1). After

Table 1
Average concentrations of the untreated and treated effluent (using the ME-nFe). Data are shown as average ± standard deviation (n = 3 for all the compounds).

Chemical	Pre-UV Effluent (ng·L^{-1})	ME-nFe treated Effluent (ng·L^{-1})
Ofloxacin (OFX)	194 ± 7	13.6 ± 0.3
Irbesartan (IRB)	11,202 ± 11	464 ± 25
Diclofenac (DCN)	1247 ± 12	78 ± 8
Clarithromycin (CLM)	34 ± 3	7 ± 1
Fluoxetine (FLX)	58 ± 4	15 ± 1
Lamotrigine (LMG)	307 ± 6	98 ± 1
Metoprolol (MTP)	195 ± 5	63 ± 4
Amisulpride (AMS)	72 ± 5	37 ± 8
Gabapentin-Lactam (GBP)	313 ± 3	256 ± 5
Propyphenazone (PHP)	9 ± 1	8 ± 1
Sulfamethoxazole (SFX)	n.d.	n.d.
Carbamazepine (CBZ)	n.d	n.d.

the ME-nFe treatment, the concentration of all compounds significantly decreased except for Gabapentin-Lactam (GBP) and Propyphenazone (PHP). The low affinity of these two compounds for the nanoparticles had already been observed in the preliminary test on the synthetic wastewater. Fig. 4A summarizes the result of the Jar test. Overall, the highest removal efficiencies were observed for Irbesartan, Ofloxacin, Diclofenac and Clarithromycin (96 ± 0%, 93 ± 1%, 94 ± 1%, and 80 ± 1%, respectively). Fluoxetine, Lamotrigine and Metoprolol removals were still significant (74 ± 3%, 68 ± 1%, 67 ± 2%, respectively). Amisulpride removal was over 45% showing the highest variability in the three replicates (48 ± 11%). This is one of the largest molecules among the studied ones, having a molecular weight of 369.5 g mol^{-1}. Its chemical properties (i.e. the combined effect of its relatively low hydrophobicity and molecular weight) may have hindered the interaction with ME-nFe nanoparticles and the diffusion through the mesopores due to steric effect (Bernal et al., 2018). But this is just a hypothesis, especially considering that Ofloxacin (having similar characteristic in terms of chemical properties) was easily removed by the nanoparticles. Pearson correlations were calculated to understand if and how the main chemical-physical properties of PhACs could have influenced the ME-nFe treatment (Fig. 4B). As expected, a significant linear correlation (p-value = 0.025) was found between the experimental data (% Removal) and the hydrophobicity of the PhACs (Log K_{OW}). This would confirm the relevance of the carbonaceous shell of the ME-nFe: while the pores of the nanoparticles are finite the most hydrophobic pollutants are the first ones to be removed through adsorption. While the role of adsorption seems evident, the ME-nFe contain zero-valent iron and iron oxides, which enhance their reductive power. Degradation processes cannot be ruled out: redox reactions could have synergistically complemented the adsorption of micropollutants on the carbonaceous shell of ME-nFe.

The results on Bresso Pre-UV effluent are noteworthy: at least a 70% removal was obtained for seven out of the ten monitored pharmaceuticals. Using the ME-nFe on this wastewater rather than the synthetic one (composed of analytical graded standards dissolved in ultrapure water) does not appear to have reduced their effectiveness. This outcome was not taken for granted, considering that the Pre- UV effluent contains a much broader range of pharmaceutical residues, organic compounds, and inorganic pollutants. At this stage, the effluent proves

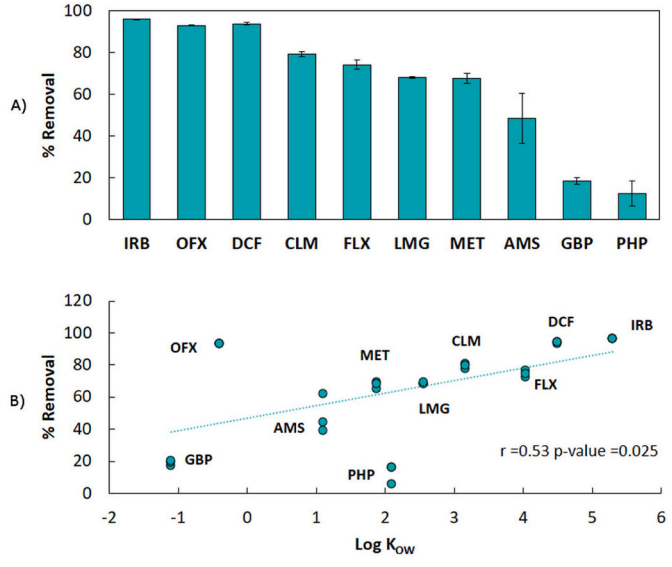

Fig. 4. A) Percent removal of Lamotrigine (LMG), Diclofenac (DCF), Fluoxetine (FLX), Metoprolol (MET), Amisulpride (AMS), Ofloxacin (OFX), Clarithromycin (CLM), Gabapentin-Lactam (GBP), Irbesartan (IRB) and Propyphenazone (PHP). Data are presented as average and standard deviations (**n = 3**); B) linear correlation between Percent removal and hydrophobicity of the PhACs.

to be free of macroscopic impurities. Its turbidity is indeed low, as well as the concentration of suspended solids (0.01 ± 0.01 g L^{-1}). This limits the undesired saturation of adsorption sites. It is important to note that the characteristics of urban wastewater, and thus of effluents, can vary, potentially influencing the performance of the nanoparticles. For instance, the role of the matrix proved significant and limiting when using ME-nFe to remove the same PhACs from the liquid phase of anaerobic sludge (centrate), where microalgae are grown to produce the nanoparticles. As visible in Fig. 5S in the Supplementary Material, only Diclofenac exhibited removal efficiencies comparable to the ones obtained in the Pre-UV Effluent test. For all other PhACs, the removal was much lower. This can be attributed to the presence of suspended and dissolved solids (0.1 ± 0.1 g L^{-1}), causing increased turbidity in the centrate, and the elevated concentration of inorganic nutrients (the concentrations of Total Ammoniacal Nitrogen and phosphates are around 250 and 10 mg L^{-1}, respectively) and organic matter (225 mg L^{-1} of chemical oxygen demand, COD). Undoubtedly, these components led to a higher and faster saturation of the nanoparticle's active sites, lowering their availability for micropollutants. However, it must be considered that ME-nFe are specifically designed for polishing the effluent at the end of the wastewater treatment train. Concerning the pre-UV test, the ME-nFe proved to be particularly effective in the lab-scale removal of Irbesartan, Ofloxacin and Diclofenac (over 90%). Literature data on their removal through conventional treatments do not always highlight such high efficiencies. According to Joss et al. and Nguyen et al. (Joss et al., 2005; Nguyen et al., 2019), Diclofenac is only partially removed by activated sludges (10–50%) while Irbesartan removal is lower than 40% (Lopez et al., 2022). As for Ofloxacin, a very high variability (0–90%) can be observed depending on different studies (Belviso et al., 2021; Estrada-Arriaga et al., 2016; Rosal et al., 2010)). Generally, the use of activated carbon or other novel adsorbents offers better options compared to biological degradation. However, research on environmentally plausible concentrations is not so widespread (at least for the category "novel adsorbent") and still focuses on isotherms, kinetics, and thermodynamic studies on highly concentrated water solutions. Genç et al. (2021) obtained an 80% removal treating a solution at 40 mg L^{-1} of Diclofenac with coconut shell-based granular activated carbon (GAC). Munoz et al. (2021) obtained an 80% removal after 5 min through the adsorption on carbon-encapsulated iron nanoparticles (CE-nFe). Moreover, the efficiency gradually increased up to 100% after 1 h. The concentration of Diclofenac (100 mg L^{-1}) was much higher than that in the Pre-UV effluent of Bresso WWTP. However, the nanoparticles used were produced through the same HTC process as in this study, albeit with a different starting biomass. ALOthman et al. (Alothman et al., 2020) obtained an 85% removal of Diclofenac from synthetic wastewater (400 μg L^{-1}) using iron composite nanoparticles (2 g L^{-1} dose and 50 min contact time). Miller et al. (2019) evaluated a wood-derived powdered activated carbon treating municipal wastewater. Diclofenac and Ofloxacin were detected among the studied micropollutants, with concentrations of 303 ng L^{-1} and 1632 ng L^{-1}, respectively. By using a 10 mg L^{-1} dose of activated carbon with a contact time of 45 min, they achieved a 30% removal for Diclofenac and 79% removal for Ofloxacin. Making comparisons with the ME-nFe of this study is not easy due to the substantial differences in adsorbent type and dosage as well as in contact times. Hydrothermal carbonization, which operates at a lower temperature, does not yield solid materials with surface areas as high as those produced through pyrolysis (which was used by (Miller et al., 2019)). Nevertheless, by increasing the adsorbent dosage during the tests, the difference in hypothetical sorption capacity appears to be mitigated. Masud et al. (2020) used reduced graphene oxide (rGO) supported nanoscale zero-valent iron (nZVI) nanohybrids (rGOnZVI) to remove micropollutant from water. The material was tested both as adsorbent and as a catalyst for Fenton-like reaction, treating a mixture of pharmaceutical compounds at a concentration of 200 μg L^{-1}. Among the studied micropollutants Diclofenac, Lamotrigine, Fluoxetine and Sulfamethoxazole were efficiently removed after 30 min

(97, 95, 98 and 74%, respectively) using 0.1 g L^{-1} of rGOnZVI. Values were even higher with the addition of H_2O_2 to perform advanced oxidation. nZVI allowed the formation of OH radicals, leading to the degradation of the above-mentioned PhACs in 10 only minutes. These seem remarkable results considering the low dosage of adsorbent needed, one order of magnitude less than the ME-nFe. However, the production of rGOnZVI through the wet chemical methods, involving $NaBH_4$ and inert atmosphere with a constant N_2 gas flow, doesn't seem particularly environmentally friendly. The pH of the pre-UV effluent (7.8 ± 0.4) is higher than the nanoparticles' point of zero charge (pHzpc $= 6.4$). Therefore, an overall negative charge is expected on the surface of the ME-nFe when dispersed in the pre-UV effluent. This aspect is crucial in understanding the interactions between nanoparticles and the different pharmaceutical compounds. Depending on their pKa and the wastewater pH, PhACs tend to dissociate to varying degrees. Fluoxetine, Metoprolol, Amisulpride, and Clarithromycin have pKa values higher than the pH of the pre-UV effluent, meaning they are primarily in their cationic forms. In these cases, the observed removal could be attributed to electrostatic attraction (Escudero-Curiel et al., 2021). The chemical structure of each compound can strongly influence the interaction with the carbonaceous shell of ME-nFe. Aromatic rings present in many pharmaceutical compounds can contribute to the adsorption mechanism through dispersive π–π coupling reactions (Román et al., 2020). More generally, the presence of OH and COOH groups (confirmed by FTIR analysis) on the carbonaceous shell of ME-nFe may be accountable for surface interactions with electron-rich regions of pollutants. This was observed in the case of nitrogen and chlorine atoms, inducing dipoles for Fluoxetine (Román et al., 2020). Irbesartan, Diclofenac, Lamotrigine, Gabapentin-Lactam, and Propyphenazone all have a pKa < pH. Irbesartan and Gabapentin-lactam are zwitterions, possessing both positive and negative charges. Due to its pKa (4.1), Diclofenac is mainly present in the anionic form in wastewater. Lamotrigine, a weak base with two protonation states, is only partially in the cationic form (pKa = 5.7) in the environment. Since electrostatic interactions are not likely to occur in those cases, the high removal of Diclofenac, Irbesartan, and Lamotrigine may also be attributed to other forces fostering adsorption, such as hydrogen bonds (H-bonds) between chemical components on the surface of the ME-nFe and the PhACs (Lach and Szymonik, 2020).

3.3. Current limitation and fate of the spent ME-nFe nanoparticles

As previously highlighted, ME-nFe nanoparticles appear particularly effective to remove highly hydrophobic PhACs. However, the sequestration of more hydrophilic molecules, such as Amisulpride, Gabapentin-Lactam, and Propyphenazone, was less effective. Among the tested micropollutants, only Ofloxacin stands out for a very high removal despite its low Log K_{OW} value. Evaluating ME-nFe across a broader spectrum of PhACs would allow for a deeper investigation. While the development of a nanoparticle management plan falls outside the scope of this study, which wanted to assess the effectiveness of ME-nFe in PhACs removal as observed with heavy metals, it is not possible to overlook this issue. The fate of spent adsorbent materials remains a critical concern. One of the advantages of iron nanoparticles is their inherent magnetism, fostering easy recovery from the treated effluent after their application. This feature enhances their control and subsequent management. Identifying strategies for nanoparticle regeneration becomes a pivotal concept to ensure their repeated use, an extended life cycle, and a reduction in the associated production costs. Existing literature displays the use of spent iron nanoparticles as catalysts in Fenton-like processes, leveraging the iron within them to start the production of radicals in the presence of hydrogen peroxide (Nieto-Sandoval et al., 2023). This process enables the chemical oxidation of the adsorbed micropollutants on the nanoparticle surface, freeing up their pores. As previously mentioned, Munoz et al. have proposed this post-treatment to regenerate carbon-encapsulated iron nanoparticles, akin to ME-nFe, yielding promising results. High-temperature heat treatments stand out as one of the most commonly employed methods for regenerating activated carbons, aiming to exceed the thermal degradation point of micropollutants and restore the adsorptive capacity of the adsorption material. However, the substantial oxygen content within the carbonaceous matrix of ME-nFe must be considered, as it could lead to additional oxidation of the iron in the nanoparticles during the treatment, altering their properties and reducing their effectiveness over time. Alternatively, chemical treatments such as desorption using solvents like methanol and ethanol could be employed for nanoparticle regeneration. Exploiting the varied affinity of different drugs and pollutants for the organic phase of the solvent might facilitate the release of the adsorbed PhACs from the active sites of the nanoparticles, restoring their adsorption capacity. The desorption mechanism would be effective until the solubility threshold of the specific pollutants is reached. It is important to note that this threshold can vary from drug to drug, leading to variable desorption efficiencies. Furthermore, the management of solvents loaded with pollutants is not of secondary importance. Some literature studies suggest that pollutant-loaded solvents could be used as co-substrates for the anaerobic digestion of municipal sludge, resulting in increased biogas production and a simultaneous partial degradation of pharmaceuticals (Granatto et al., 2020). Establishing a sustainable post-use strategy could really enhance the competitiveness of this technology for wastewater treatment.

4. Conclusion

ME-nFe, formed by a carbonaceous shell coating zero-valent iron and iron oxide nanoparticles, proved to be an effective adsorbent for pharmaceutical compounds. Produced through hydrothermal carbonization of microalgal biomass and iron nitrate, this method is both environmentally friendly and energetically efficient, representing an innovative option for adsorbent production. The obtained nanoparticles were tested at the laboratory scale, treating both synthetic solutions and real municipal pre-UV effluent containing environmentally relevant concentrations of PhACs. Despite the relatively modest specific surface area (117 m^2 g^{-1}), the mesoporous structure of ME-nFe and their high reactivity due to iron components proved effective, particularly against seven of the tested PhACs. Moreover, the magnetic properties of the nanoparticles facilitate easy recovery, distinguishing it from powdered activated carbons and enhancing practicality in wastewater treatment applications. A direct and significant correlation between the experimental data and the hydrophobicity of PhACs was observed, suggesting that the Me-nFe could be particularly useful for removing those pollutants but is probably not as effective for more hydrophilic compounds. Preliminary tests on synthetic solutions allowed to understand that the ME-nFe were more effective when used at 1 g L^{-1} dose and 2 min contact time, minimizing agglomeration and desorption phenomena. When used to treat a municipal effluent, the ME-nFe were even more effective particularly toward Irbesartan, Ofloxacin and Diclofenac (over 90% removals) while Clarithromycin, Fluoxetine, Lamotrigine and Metoprolol removal ranged from 65 to 80%. The obtained results are certainly promising, highlighting the potential of ME-nFe for wastewater treatment, particularly in contexts where locally produced algal biomass can be used. Developing strategies for the regeneration of spent nanoparticles could make this approach more attractive from an economic perspective while increasing the environmental sustainability of municipal WWTPs.

CRediT authorship contribution statement

Marco Mantovani: Writing – original draft, Methodology, Investigation, Formal analysis, Data curation, Conceptualization. **Elena Collina:** Writing – review & editing, Supervision, Conceptualization. **Elena Passalacqua:** Writing – review & editing, Formal analysis. **Marina Lasagni:** Writing – review & editing, Supervision, Conceptualization. **Valeria Mezzanotte:** Writing – review & editing, Supervision,

Methodology, Conceptualization.

Declaration of competing interest

The authors declare that they have no known competing financial interests or personal relationships that could have appeared to influence the work reported in this paper.

Data availability

Data will be made available on request.

Acknowledgements

PerFORM WATER 2030, funded by the European Community through FESR (Fondo Europeo di Sviluppo Regionale), supported the study. The authors would like to acknowledge Bresso-Seveso Sud WWTP and AMIACQUE (CAP Holding) and all their workers for hosting the experimentation and for their help. We are also thankful to SEAM engineering for the construction of the raceway and to all the students who worked on this project.

Appendix A. Supplementary data

Supplementary data to this article can be found online at https://doi.org/10.1016/j.jenvman.2024.122171.

References

Adeleye, A.S., Xue, J., Zhao, Y., Taylor, A.A., Zenobio, J.E., Sun, Y., Han, Z., Salawu, O. A., Zhu, Y., 2022. Abundance, fate, and effects of pharmaceuticals and personal care products in aquatic environments. J. Hazard Mater. https://doi.org/10.1016/j.jhazmat.2021.127284.

Alothman, Z.A., Badjah, A.Y., Alharbi, O.M.L., Ali, I., 2020. Synthesis of chitosan composite iron nanoparticles for removal of diclofenac sodium drug residue in water. Int. J. Biol. Macromol. 159, 870–876. https://doi.org/10.1016/j.ijbiomac.2020.05.154.

APHA/AWWA/WEF, 2012. Standard methods for the examination of water and wastewater. Stand. Methods 541, 9780875532356.

Belviso, C., Guerra, G., Abdolrahimi, M., Peddis, D., Maraschi, F., Cavalcante, F., Ferretti, M., Martucci, A., Sturini, M., 2021. Efficiency in ofloxacin antibiotic water remediation by magnetic zeolites formed combining pure sources and wastes. Processes 9. https://doi.org/10.3390/pr9122137.

Bernal, V., Giraldo, L., Moreno-Piraján, J.C., 2018. Physicochemical Properties of Activated Carbon: Their Effect on the Adsorption of Pharmaceutical Compounds and Adsorbate–Adsorbent Interactions, vol. 4, p. 62. https://doi.org/10.3390/c4040062. C.

Bhadra, B.N., Seo, P.W., Jhung, S.H., 2016. Adsorption of diclofenac sodium from water using oxidized activated carbon. Chem. Eng. J. 301 https://doi.org/10.1016/j.cej.2016.04.143.

Bhattarai, A., Khanal, M., Rai, D., Khanal, R., 2020. Determination of point zero charge (PZC) of homemade charcoals of shorea robusta (sakhuwa) and pinus roxburghii (salla). Int. J. Eng. Res. Technol. 9 https://doi.org/10.17577/IJERTV9IS100046.

Bollmann, A.F., Seitz, W., Prasse, C., Lucke, T., Schulz, W., Ternes, T., 2016. Occurrence and fate of amisulpride, sulpiride, and lamotrigine in municipal wastewater treatment plants with biological treatment and ozonation. J. Hazard Mater. 320 https://doi.org/10.1016/j.jhazmat.2016.08.022.

Calderon, B., Smith, F., Aracil, I., Fullana, A., 2018. Green synthesis of thin shell carbon-encapsulated iron nanoparticles via hydrothermal varbonization. ACS Sustain. Chem. Eng. 13, 24. https://doi.org/10.1021/acssuschemeng.8b01416.

Dolatabadi, M., Akbarpour, R., Ahmadzadeh, S., 2022. Catalytic ozonation process using ZnO/Fe2 O3 nanocomposite for efficient removal of captopril from aqueous solution. Anal. Methods Environ. Chem. J. 5, 31–39. https://doi.org/10.24200/amecj.v5.i03.197.

Escudero-Curiel, S., Penelas, U., Sanromán, M.Á., Pazos, M., 2021. An approach towards Zero-Waste wastewater technology: fluoxetine adsorption on biochar and removal by the sulfate radical. Chemosphere 268. https://doi.org/10.1016/j.chemosphere.2020.129318.

Estrada-Arriaga, E.B., Cortés-Muñoz, J.E., González-Herrera, A., Calderón-Mólgora, C.G., de Lourdes Rivera-Huerta, M., Ramírez-Camperos, E., Montellano-Palacios, L., Gelover-Santiago, S.L., Pérez-Castrejón, S., Cardoso-Vigueros, L., Martín-Domínguez, A., García-Sánchez, L., 2016. Assessment of full-scale biological nutrient removal systems upgraded with physico-chemical processes for the removal of emerging pollutants present in wastewaters from Mexico. Sci. Total Environ. 571 https://doi.org/10.1016/j.scitotenv.2016.07.118.

Frascaroli, G., Reid, D., Hunter, C., Roberts, J., Helwig, K., Spencer, J., Escudero, A., 2021. Pharmaceuticals in wastewater treatment plants: a systematic review on the substances of greatest concern responsible for the development of antimicrobial resistance. Appl. Sci. 11 https://doi.org/10.3390/app11156670.

Fronczak, M., Łabędź, O., Kaszuwara, W., Bystrzejewski, M., 2018. Corrosion resistance studies of carbon-encapsulated iron nanoparticles. J. Mater. Sci. 53, 3805–3816. https://doi.org/10.1007/s10853-017-1793-z.

Gautam, M.K., Mondal, T., Nath, R., Mahajon, B., Chincholikar, M., Bose, A., Das, D., Das, R., Mondal, S., 2024. Harnessing Activated Hydrochars: A Novel Approach for Pharmaceutical Contaminant Removal.

Genç, N., Durna, E., Erkişi, E., 2021. Optimization of the adsorption of diclofenac by activated carbon and the acidic regeneration of spent activated carbon. Water Sci. Technol. 83 https://doi.org/10.2166/wst.2020.577.

Granatto, C.F., Grosseli, G.M., Sakamoto, I.K., Fadini, P.S., Varesche, M.B.A., 2020. Methanogenic potential of diclofenac and ibuprofen in sanitary sewage using metabolic cosubstrates. Sci. Total Environ. 742, 140530 https://doi.org/10.1016/j.scitotenv.2020.140530.

Joss, A., Keller, E., Alder, A.C., Göbel, A., McArdell, C.S., Ternes, T., Siegrist, H., 2005. Removal of pharmaceuticals and fragrances in biological wastewater treatment. Water Res. 39 https://doi.org/10.1016/j.watres.2005.05.031.

Lach, J., Szymonik, A., 2020. Adsorption of diclofenac sodium from aqueous solutions on commercial activated carbons. Desalin. Water Treat. 186 https://doi.org/10.5004/dwt.2020.25567.

Liu, T., Aniagor, C.O., Ejimofor, M.I., Menkiti, M.C., Tang, K.H.D., Chin, B.L.F., Chan, Y. H., Yiin, C.L., Cheah, K.W., Ho Chai, Y., Lock, S.S.M., Yap, K.L., Wee, M.X.J., Yap, P. S., 2023. Technologies for removing pharmaceuticals and personal care products (PPCPs) from aqueous solutions: recent advances, performances, challenges and recommendations for improvements. J. Mol. Liq. https://doi.org/10.1016/j.molliq.2022.121144.

Lopez, F.J., Pitarch, E., Botero-Coy, A.M., Fabregat-Safont, D., Ibáñez, M., Marin, J.M., Peruga, A., Ontañón, N., Martínez-Morcillo, S., Olalla, A., Valcárcel, Y., Varó, I., Hernández, F., 2022. Removal efficiency for emerging contaminants in a WWTP from Madrid (Spain) after secondary and tertiary treatment and environmental impact on the Manzanares River. Sci. Total Environ. 812 https://doi.org/10.1016/j.scitotenv.2021.152567.

Luo, Q., Wang, J., Wang, J.H., Shen, Y., Yan, P., Chen, Y.P., Zhang, C.C., 2019. Fate and occurrence of pharmaceutically active organic compounds during typical pharmaceutical wastewater treatment. J. Chem. 2019 https://doi.org/10.1155/2019/2674852.

Mantovani, M., Collina, E., Lasagni, M., Marazzi, F., Mezzanotte, V., 2023. Production of microalgal-based carbon encapsulated iron nanoparticles (ME-nFe) to remove heavy metals in wastewater. Environ. Sci. Pollut. Res. 30 https://doi.org/10.1007/s11356-022-22506-x.

Mantovani, M., Rossi, S., Ficara, E., Collina, E., Marazzi, F., Lasagni, M., Mezzanotte, V., 2024. Removal of pharmaceutical compounds from the liquid phase of anaerobic sludge in a pilot-scale high-rate algae-bacteria pond. Sci. Total Environ. 908, 167881 https://doi.org/10.1016/j.scitotenv.2023.167881.

Masud, A., Chavez Soria, N.G., Aga, D.S., Aich, N., 2020. Adsorption and advanced oxidation of diverse pharmaceuticals and personal care products (PPCPs) from water using highly efficient rGO-nZVI nanohybrids. Environ. Sci. Water Res. Technol. 6, 2223–2238. https://doi.org/10.1039/d0ew00140f.

Mezzanotte, V., Romagnoli, F., Ievina, B., Mantovani, M., Invernizzi, M., Ficara, E., Collina, E., 2022. LCA of zero valent iron nanoparticles encapsulated in algal biomass for polishing treated effluents. Environ. Clim. Technol. 26, 1196–1208. https://doi.org/10.2478/rtuect-2022-0090.

Miller, T.H., Ng, K.T., Bury, S.T., Bury, S.E., Bury, N.R., Barron, L.P., 2019. Biomonitoring of pesticides, pharmaceuticals and illicit drugs in a freshwater invertebrate to estimate toxic or effect pressure. Environ. Int. 129, 595–606. https://doi.org/10.1016/J.ENVINT.2019.04.038.

Mirzaei, A., Chen, Z., Haghighat, F., Yerushalmi, L., 2017. Removal of pharmaceuticals from water by homo/heterogonous Fenton-type processes – a review. Chemosphere. https://doi.org/10.1016/j.chemosphere.2017.02.019.

Munoz, M., Nieto-Sandoval, J., Álvarez-Torrellas, S., Sanz-Santos, E., Calderón, B., de Pedro, Z.M., Larriba, M., Fullana, A., García, J., Casas, J.A., 2021. Carbon-encapsulated iron nanoparticles as reusable adsorbents for micropollutants removal from water. Sep. Purif. Technol. 257, 117974 https://doi.org/10.1016/j.seppur.2020.117974.

Nabatian, E., Dolatabadi, M., Ahmadzadeh, S., 2022. Application of experimental design methodology to optimize acetaminophen removal from aqueous environment by magnetic chitosan@multi-walled carbon nanotube composite: isotherm, kinetic, and regeneration studies. Anal. Methods Environ. Chem. J. 5, 61–74. https://doi.org/10.24200/amecj.v5.i01.168.

Nakarmi, K.J., Daneshvar, E., Eshaq, G., Puro, L., Maiti, A., Nidheesh, P.V., Wang, H., Bhatnagar, A., 2022. Synthesis of biochar from iron-free and iron-containing microalgal biomass for the removal of pharmaceuticals from water. Environ. Res. 214, 114041 https://doi.org/10.1016/j.envres.2022.114041.

Nguyen, L.N., Nghiem, L.D., Pramanik, B.K., Oh, S., 2019. Cometabolic biotransformation and impacts of the anti-inflammatory drug diclofenac on activated sludge microbial communities. Sci. Total Environ. 657 https://doi.org/10.1016/j.scitotenv.2018.12.094.

Nieto-Sandoval, J., Morabet, F. El, Munoz, M., Lopez-Arago, N., de Pedro, Z.M., Casas, J. A., 2023. In-situ regeneration of a novel Fe3O4/GAC adsorbent for micropollutants removal in a continuous fixed-bed. J. Hazard. Mater. Adv. 10, 100267 https://doi.org/10.1016/j.hazadv.2023.100267.

Noreen, S., Mustafa, G., Ibrahim, S.M., Naz, S., Iqbal, M., Yaseen, M., Javed, T., Nisar, J., 2020. Iron oxide (Fe2O3) prepared via green route and adsorption efficiency evaluation for an anionic dye: kinetics, isotherms and thermodynamics studies. J. Mater. Res. Technol. 9 https://doi.org/10.1016/j.jmrt.2020.02.047.

Noudeh, G.D., Asdaghi, M., Noudeh, N.D., Dolatabadi, M., Ahmadzadeh, S., 2023. Response surface modeling of ceftriaxone removal from hospital wastewater. Environ. Monit. Assess. 195, 1–12. https://doi.org/10.1007/s10661-022-10808-z.

Olusegun, S.J., Souza, T.G.F., Souza, G. de O., Osial, M., Mohallem, N.D.S., Ciminelli, V. S.T., Krysinski, P., 2023. Iron-based materials for the adsorption and photocatalytic degradation of pharmaceutical drugs: a comprehensive review of the mechanism pathway. J. Water Process Eng. 51, 103457 https://doi.org/10.1016/j.jwpe.2022.103457.

Rodríguez-Serin, H., Gamez-Jara, A., De La Cruz-Noriega, M., Rojas-Flores, S., Rodriguez-Yupanqui, M., Gallozzo Cardenas, M., Cruz-Monzon, J., 2022. Literature review: evaluation of drug removal techniques in municipal and hospital wastewater. Int. J. Environ. Res. Public Health. https://doi.org/10.3390/ijerph192013105.

Román, S., Nabais, J.M.V., Ledesma, B., Laginhas, C., Titirici, M.M., 2020. Surface interactions during the removal of emerging contaminants by hydrochar-based adsorbents. Molecules 25. https://doi.org/10.3390/molecules25092264.

Rosal, R., Rodríguez, A., Perdigón-Melón, J.A., Petre, A., García-Calvo, E., Gómez, M.J., Agüera, A., Fernández-Alba, A.R., 2010. Occurrence of emerging pollutants in urban wastewater and their removal through biological treatment followed by ozonation. Water Res. 44 https://doi.org/10.1016/j.watres.2009.07.004.

Rossi, S., Mantovani, M., Marazzi, F., Bellucci, M., Casagli, F., Mezzanotte, V., Ficara, E., 2023. Microalgal cultivation on digestate: process efficiency and economics. Chem. Eng. J. 460, 141753 https://doi.org/10.1016/j.cej.2023.141753.

Silori, R., Tauseef, S.M., 2021. A review of the occurrence of pharmaceutical compounds as emerging contaminants in treated wastewater and aquatic environments. Curr. Pharm. Anal. 18 https://doi.org/10.2174/1573412918666211119142030.

Skandalis, N., Maeusli, M., Papafotis, D., Miller, S., Lee, B., Theologidis, I., Luna, B., 2021. Environmental spread of antibiotic resistance. Antibiotics 10. https://doi.org/10.3390/antibiotics10060640.

Tua, C., Ficara, E., Mezzanotte, V., Rigamonti, L., 2021. Integration of a side-stream microalgae process into a municipal wastewater treatment plant: a life cycle analysis. J. Environ. Manage. 279, 111605 https://doi.org/10.1016/j.jenvman.2020.111605.

Wang, T., Zhai, Y., Zhu, Y., Li, C., Zeng, G., 2018. A review of the hydrothermal carbonization of biomass waste for hydrochar formation: process conditions, fundamentals, and physicochemical properties. Renew. Sustain. Energy Rev. https://doi.org/10.1016/j.rser.2018.03.071.

Xiao, Y., Hill, J.M., 2017. Impact of pore size on Fenton oxidation of methyl orange adsorbed on magnetic carbon materials: trade-off between capacity and regenerability. Environ. Sci. Technol. 51 https://doi.org/10.1021/acs.est.7b00089.

Zou, Y., Wang, X.X., Khan, A., Wang, P., Liu, Y., Alsaedi, A., Hayat, T., Wang, X.X., 2016. Environmental remediation and application of nanoscale zero- valent iron and its composites for the removal of heavy metal ions: a review. Environ. Sci. Technol. 50, 7290–7304. https://doi.org/10.1021/acs.est.6b01897.